VIRUS EVOLUTION

Virus Evolution, 2022, **7(2)**, 1–11

DOI: https://doi.org/10.1093/ve/veab106

Advance access publication date: 23 December 2021

Research Article

High recombination rate of hepatitis C virus revealed by a green fluorescent protein reconstitution cell system

Andrea Galli,*,† Ulrik Fahnøe, and Jens Bukh*,‡

Copenhagen Hepatitis C Program (CO-HEP), Department of Infectious Diseases, Copenhagen University Hospital, Kettegaard Alle 30, 2650, Hvidovre and Department of Immunology and Microbiology, Faculty of Health and Medical Sciences, University of Copenhagen, Blegdamsvej 3B, 2200, Copenhagen Denmark

†https://orcid.org/0000-0002-4404-430X

‡https://orcid.org/0000-0002-7815-4806

*Corresponding authors: E-mail: andrea.galli@regionh.dk; jbukh@sund.ku.dk

Abstract

Genetic recombination is an important evolutionary mechanism for RNA viruses and can facilitate escape from immune and drug pressure. Recombinant hepatitis C virus (HCV) variants have rarely been detected in patients, suggesting that HCV has intrinsic low recombination rate. Recombination of HCV has been demonstrated *in vitro* between non-functional genomes, but its frequency and relevance for viral evolution and life cycle has not been clarified. We developed a cell-based assay to detect and quantify recombination between fully viable HCV genomes, using the reconstitution of green fluorescent protein (GFP) as a surrogate marker for recombination. Here, two GFP-expressing HCV genomes carrying different inactivating GFP mutations can produce a virus carrying a functional GFP by recombining within the GFP region. Generated constructs allowed quantification of recombination rates between markers spaced 603 and 553 nucleotides apart by flow cytometry and next-generation sequencing (NGS). Viral constructs showed comparable spread kinetics and reached similar infectivity titers in Huh7.5 cells, allowing their use in co-transfections and co-infections. Single-cycle co-transfection experiments, performed in CD81-deficient S29 cells, showed GFP expression in double-infected cells, demonstrating genome mixing and occurrence of recombination. Quantification of recombinant genomes by NGS revealed an average rate of 6.1 per cent, corresponding to 49 per cent of maximum detectable recombination (MDR). Experiments examining recombination during the full replication cycle of HCV, performed in Huh7.5 cells, demonstrated average recombination rates of 5.0 per cent (40.0 per cent MDR) and 3.6 per cent (28.8 per cent MDR) for markers spaced by 603 and 553 nucleotides, respectively, supporting a linear relationship between marker distance and recombination rates. First passage infections using recombinant virus supernatant resulted in comparable recombination rates of 5.9 per cent (47.2 per cent MDR) and 3.5 per cent (28.0 per cent MDR), respectively, for markers spaced by 603 and 553 nucleotides. We developed a functional cell-based assay that, to the best of our knowledge, allows for the first time detailed quantification of recombination rates using fully viable HCV constructs. Our data indicate that HCV recombines at high frequency between highly similar genomes and that the frequency of recombination increases with the distance between marker sites. These results have implication for our understanding of HCV evolution and emphasize the importance of recombination in the reassortment of mutations in the HCV genome.

Key words: HCV; recombination; GFP; RNA virus; next-generation sequencing; cell culture system; flow cytometry

1. Introduction

Genetic recombination is a widespread evolutionary mechanism across all life domains, allowing the rapid exchange of large portions of genetic material between genomes (Lai 1992; Stapley et al. 2017). In the context of viral infections, recombination has important implications for the study of viral evolution, monitoring of viral molecular epidemiology, and development of drug and immune escape variants (Worobey and Holmes 1999). Viral genetic recombination has important implications for the study of viral origin and evolution, which is relevant to understand the molecular epidemiology of viruses and can accelerate the development of viral strains carrying multiple mutations that confer antiviral resistance or immune escape (Uzcategui et al. 2001; Rambaut et al. 2004; Zhang, Yap, and Danchin 2005; Paprotka et al. 2011). Viral recombination has been investigated in several RNA viruses and retroviruses, leading to a better understanding of the molecular mechanisms regulating its occurrence during infection (Galli and Bukh 2014).

Hepatitis C virus (HCV) is a member of the *Flaviviridae* family of RNA viruses, further classified as the prototype member in the genus *Hepacivirus* (Bukh 2016). It has a single-stranded positive-sense RNA genome of about 9,600 nucleotides, which encodes a single polyprotein that is further processed by viral and cellular proteases into three structural proteins (core and envelope glycoproteins E1 and E2), as well as seven nonstructural proteins (p7, NS2, NS3, NS4A and B, and NS5A and B). Due to its high

genetic heterogeneity HCV is classified into 8 genotypes and >90 subtypes, differing at least 25 per cent and 15 per cent at the nucleotide level, respectively (Smith et al. 2014; Borgia et al. 2018). Despite the large number of HCV genotypes and subtypes, circulating recombinant forms (CRFs) have been described relatively seldom in patients (Kalinina et al. 2002; Colina et al. 2004; Cristina and Colina 2006; Kageyama et al. 2006; Noppornpanth et al. 2006; Legrand-Abravanel et al. 2007; Ross et al. 2008; Moreno et al. 2009; Lee et al. 2010; Bhattacharya et al. 2011; Calado et al. 2011; Yokoyama et al. 2011; Hoshino et al. 2012; Shi et al. 2012). This is in stark contrast to highly recombinogenic retroviruses, such as HIV-1, for which the number of described CRFs is in excess of 100 (Chang et al. 2020), suggesting that HCV might have intrinsic reduced recombination capacity.

Studies of HCV recombination in chimpanzees showed detectable recombination events between strains, with an estimated frequency of 3×10^{-5} crossovers/nucleotide (Gao et al. 2007). More recently, investigation of recombination using replicon systems and human cell culture systems indicated that HCV could recombine efficiently *in vitro*, although at lower frequencies (Reiter et al. 2011; Scheel et al. 2013). Although not directly comparable with replicative recombination, the predominant mechanism driving HIV-1 recombination, these results seemed to confirm that HCV has the capability to recombine, albeit at lower frequency than other RNA viruses. Recombination has been observed in members of the other three genera within the *Flaviviridae* family, represented by pestivirus bovine viral diarrhea virus (BVDV), flavivirus dengue virus, and pegivirus GB virus C (Worobey, Rambaut, and Holmes 1999; Fricke, Gunn, and Meyers 2001; Worobey and Holmes 2001). In particular, BVDV relies on a recombination mechanism to produce its cytopathogenic biotype and has been shown to recombine by both homologous and non-homologous recombination (Baroth et al. 2000; Fricke, Gunn, and Meyers 2001).

To better understand the role of replicative recombination in HCV, we developed a cell-culture-based assay to quantify recombination events during replication of fully viable HCVs. Similar systems have been used extensively for the study of retroviral recombination (Rhodes et al. 2005; Galli et al. 2010; Rawson et al. 2018). To the best of our knowledge, this is the first study that quantitatively addresses replicative recombination in HCV infection. We applied the system to clarify recombination frequencies in both single-cycle and normal infection conditions.

2. Materials and methods

2.1 Cell culture, transfections, and infections

Cells from the human hepatoma cell line Huh7.5 were maintained in dulbecco's modified eagle medium (DMEM) supplemented with 10 per cent fetal bovine serum, penicillin 100 U/ml, and streptomycin 100 μg/ml, as previously described (Galli, Ramirez, and Bukh 2021). A clone of Huh7 cells deficient for the CD81 receptor, the S29 cell line (Russell et al. 2008), was maintained as Huh7.5 cells.

For transfections, cells were plated in 6-well plates at a density of 4×10^5 cells/well and incubated for 24 h at 37°C in humidified incubators. *In vitro* transcribed viral RNA was then mixed with 5 μl Lipofectamine 2000 (Thermo Fisher) in 500 μl Opti-MEM (Thermo Fisher) and incubated at room temperature in the dark. Cell medium was replaced with 2 ml Opti-MEM medium and the RNA–Lipofectamine transfection mix was added to the cells dropwise. For infections, 4×10^5 cells/well were plated in 6-well plates and inoculated with cell cultured HCV 24 h post-seeding at the indicated multiplicity of infection (MOI).

Both transfected and infected cells were then split into 25 ml flasks after 24 h incubation and subsequently every 2–3 days, when viral supernatants were collected and stored at −80°C. Viral spread was monitored by immunostaining as previously described and detailed in the Microscopy sub-section (Galli et al. 2018; Galli, Ramirez, and Bukh 2021).

2.2 Viral constructs

Viral constructs were built using the full-length J6/JFH1 backbone (Lindenbach et al. 2005) using standard molecular cloning techniques (Fig. 1A). The NS5A region carrying green fluorescent protein (GFP) and a downstream 40 amino acid deletion (d40) was obtained from 2a(J6)-EGFPΔ40 (Gottwein et al. 2011), whereas E2 tagged with flag tag was subcloned from J6/JFH1$_{flag}$ (Prentoe and Bukh 2011). To identify viable GFP-inactivating mutations, selected changes (Zacharias and Tsien 2006) were initially cloned into pGFP-N1 (Clontech) using QuikChange Lightning kit (Agilent) following manufacturer's recommendations. The GFP fluorescence levels of the different clones were then visually evaluated by fluorescence microscopy to identify mutations able to fully abrogate GFP fluorescence.

To generate the J6/JFH1-FDG construct, fully functional GFP was cloned into J6/JFH1 at the same location as 2a(J6)-EGFPΔ40 and then the d40 deletion was cloned from 2a(J6)-EGFPΔ40 downstream of GFP, generating the intermediate construct J6/JFH1-DG. Subsequently, E2$_{flag}$ was subcloned from J6/JFH1$_{flag}$ into J6/JFH1-DG, producing J6/JFH1-FDG. The flag-tag region of J6/JFH1-FDG was then replaced with myc tag by fusion polymerase chain reaction (PCR), resulting in J6/JFH1-MDG. The appropriate mutated GFP regions were then subcloned from the mutated pGFP-N1 plasmids into either J6/JFH1-MDG or J6/JFH1-FDG, replacing the functional GFP, leading to J6/JFH1-MD0, FD5, and FD6. J6/JFH1-Flag and J6/JFH1-Myc, carrying E2$_{flag}$ and E2$_{myc}$, respectively, were produced by cloning the E2-tag region from J6/JFH1-FDG or MDG into J6/JFH1.

Viral RNA for transfections was produced by linearizing construct plasmids with XbaI restriction enzyme (Thermo Fisher) and transcribing RNA *in vitro* using T7 RNA polymerase (Thermo Fisher) according to manufacturer's recommendations. The synthesis of viral RNA was confirmed by agarose gel electrophoresis, and RNA was used directly for transfection.

2.3 Infectivity estimation

Infectivity was quantified as previously described (Mejer et al. 2020). Briefly, Huh7.5 cells were plated on 96-well plates at 6,000 cells/well and were infected 24 h post-seeding with serial dilutions of filtered culture supernatants, in triplicates. Cells were fixed 48 h post-infection with methanol, treated with 3 per cent hydrogen peroxide, and stained using anti-NS5A (9E10; a gift from C. M. Rice) (Lindenbach et al. 2005) and anti-Core (C7-50; Abcam) as primary antibodies. Secondary staining with anti-mouse antibody conjugated to horseradish peroxidase (GE Life Science), followed by incubation with 3,3′-diaminobenzidine (DAB) substrate (Dako North America Inc), produced a color reaction in infected cells. Plates were scanned to count focus-forming units (FFU) using an Immunospot plate reader (CTL-Europe). Triplicate wells were averaged after removal of background, allowing calculation of the mean infectivity as Log_{10} FFU/ml.

2.4 Flow cytometry

During flow cytometry experiments, cells were harvested at culture split concomitantly with viral supernatants collection

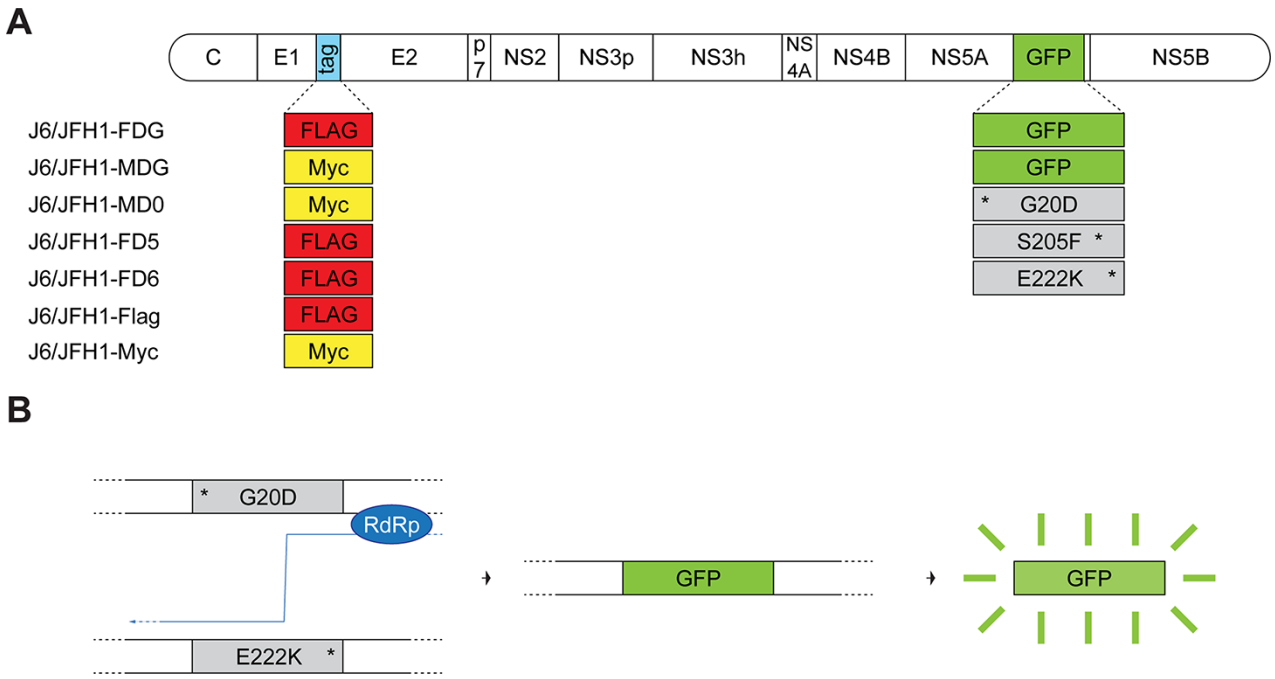

Figure 1. Experimental design of the detection assay. A) Schematic representation of HCV recombinant constructs utilized in this study. The genetic structure of the HCV open reading frame is depicted with the protein-coding regions illustrated to approximate scale. The tag box in blue shows where either flag or myc tags were introduced and fused to the E2 protein, as indicated in the lower portion of Panel A. The GFP box in green indicates where either functional or mutated GFP genes were introduced within the NS5A coding region, as indicated in the respective boxes in the lower section of Panel A. Construct names indicated on the left-hand side of Panel A are used to recapitulate the tags and GFP introduced in each construct. B) Mechanistic representation of the assay detection principle. As the RNA-dependent-RNA-polymerase encoded by HCV (NS5B) synthesizes genomic RNA, it can switch template and proceed with synthesis on the new template. When the template switch occurs between GFP mutations in the correct sequence, exemplified in the figure from MD0 to FD6, a genome carrying functional GFP gene is produced. Upon transcription and translation of the recombinant genome, GFP signal is released in the infected cell.

and processed immediately for flow cytometry analysis. Briefly, after trypsinization the cells were washed in 1× phosphate buffered saline (PBS), fixed with 4 per cent formaldehyde for 10 min, and washed again in PBS. Cells were then incubated for blocking/staining/permeabilization using 1× PBS buffer containing 0.5 per cent saponin, 1 per cent bovine serum albumin (BSA), 0.2 per cent skimmed milk, and the appropriate antibodies for 1 h at room temperature. After washing with PBS, cells were run on an LSR Fortessa flow cytometer using FACSDiva 8 (Becton Dickinson). Experiments were conducted using combinations of two antibodies: mouse anti-flag conjugated with phycoerythrin (αFlag-PE; 637310, Biolegend) and mouse anti-myc conjugated to AlexaFluor647 (αMyc-647; 2233S, Cell Signaling Tech.); detection was performed using fluorescein (FITC) channel for GFP, phycoerythrin (PE) channel for the flag tag, and allophycocyanin (APC) channel for myc tag, including proper single-staining controls for calibration and compensation. Data analysis was performed using FlowJo v10 (Becton Dickinson). Myc- and flag-positive populations were enumerated directly after compensation by gating for FITC and PE, respectively. Double-infected populations were calculated by performing a binary intersection function of the FITC and PE gated populations; recombinant-containing cells were counted by gating for GFP signal in the double-infected population.

2.5 Microscopy

Cells were plated on 12-well chamber slides (Ibidi) to routinely monitor viral spread, assess constructs viability, and verify expression of inserted sequences. Slides were processed 24 h after plating as previously described (Galli, Ramirez, and Bukh 2021). Briefly, cells were fixed in 4 per cent formaldehyde for 10 min and washed in 1× PBS three times. Staining and permeabilization were conducted in 1× PBS containing 0.5 per cent saponin, 1 per cent BSA, 0.2 per cent skimmed milk, and primary antibodies overnight at 4°C.

For routine cell culture staining, the primary antibodies used were mouse anti-Core (C7-50; Abcam) at 1:2,000 dilution followed by secondary incubation in PBS for 1 h with AlexaFluor488 anti-mouse (1:1,000 dilution) and Hoechst 33342 (1:5,000 dilution). After the final wash, cells were mounted using Prolong Diamond (Thermo Fisher) and cured for 24 h in the dark, before being analyzed on a Zeiss Axiovert microscope using a 20× dry objective and Colibri LED illumination system. The percentage of infected cells was visually estimated.

To assess expression of the inserted sequences, primary antibodies used were mouse anti-Core (C7-50; Abcam) at 1:500 dilution, rabbit anti-flag tag (ab236777; Abcam) at 1:500 dilution, and rabbit anti-myc tag (Biolegend) at 1:1,000 dilution. After wash, cells were stained with AlexaFluor555 anti-mouse (Thermo Fisher) and AlexaFluor647 anti-rabbit (Thermo Fisher) at 1:1,000 dilution and counter-stained with Hoechst 33342 at 1:5,000 dilution. After washing, slides were mounted using Prolong Diamond (Thermo Fisher) and cured for 24 h in the dark. Epi-fluorescence imaging was performed on a Zeiss AxioObserver Z1, using a 40× numerical aperture (NA) 0.6 oil immersion objective, using an Andor Ixon Ultra 897 camera at 512 × 512 pixel resolution, resulting in a final pixel size of 63 nm. Multichannel images were acquired and processed using Zeiss Zen 2.0 software. Image composition was done in Adobe Illustrator.

2.6 Viral RNA purification and sequencing

Viral supernatants were processed as previously described (Fahnøe and Bukh 2019; Mejer et al. 2020). Briefly, 250 μl of sample were suspended in 750 μl of TRIzol LS (Thermo Fisher Scientific), and RNA was extracted using Phase lock gel tubes (Quantabio) followed by RNA Clean & Concentrator-5 (Zymo Research). Reverse transcription of full-length open reading frame (ORF) HCV RNA was performed with Maxima H minus reverse transcriptase (Thermo Scientific) with RNasin Plus RNase inhibitor (Promega) at 50°C for 120 min followed by 5 min at 85°C using genotype 2a specific primer (AGCTATGGAGTGTACCTAGTGT). Complementary DNA (cDNA) was treated with RNase H (20 min at 37°C) and amplified (35 cycles at 98°C for 10 s, 65°C for 10 s, and 72°C for 8 m) using Hot Start High-Fidelity Q5 DNA Polymerase (New England Biolabs) with genotype 2a specific forward (CTTGCGAGTGCCCCGGGAGG) and reverse (TGGAGTGTACCTAGTGTGTGCCGCTC) primers. Four separate PCRs of each sample were pooled, cleaned (DNA Clean & Concentrator, Zymo Research), and evaluated for size and purity on 1 per cent agarose gels stained with GelRed (Biotium). DNA concentration was estimated using a Nanodrop reader (Thermo Fisher) and PCR products were full-length sequenced using an array of 24 overlapping primers by Macrogen. Sequence analysis was performed using Sequencher 5.4.6 (Genecodes Corp.).

2.7 Analysis of GFP recombination by NGS

Viral RNA was extracted and reverse transcribed as described above for viral RNA purification and sequencing. To assess the impact of reverse transcriptase (RT)-PCR and next-generation sequencing (NGS)-PCR induced recombination, we included at this stage a control consisting of a 1:1 mix of J6/JFH1-MD0 and J6/JFH1-FD6 RNA that was processed in parallel with the supernatant samples. A 786-nucleotide region encompassing the GFP gene was then amplified directly from cDNA using specific forward (CTCGAGGGCTTAAGTGGAGGGATG) and reverse (AGACTCCAGGTCCGGATCTCCAG) primers flanking the protein-coding region. Four separate PCRs of each sample were pooled, gel purified from 1 per cent agarose gels (Zymoclean Gel DNA Recovery Kit, Zymo Research), and quantified on a Qubit Fluorometer (Thermo Fisher Scientific). Libraries for NGS were prepared with the NEBNext Ultra II DNA kit on 50 ng of gel-extracted PCR product, no fragmentation was performed, the products were size selected (>500 bases) using Ampure XP beads (Beckman Coulter) and multiplexed with dual indexes (New England Biolabs). The size and concentration of the library preparations were quantified on a 2100 Bioanalyzer (Agilent Technologies), and library preparations diluted to 4 nM were pooled for NGS using the Illumina MiSeq platform and the v2 500 cycle kit. Linkage of inactivating mutations located at the ends of the GFP coding region was calculated using an in-house developed protocol, returning an estimate of recombination frequency within the GFP region (Jensen et al. 2019). Briefly, reads were mapped to the sequence fragment corresponding to the RT-PCR product using BWA MEM and Samtools. Inactivating mutation sites located in the forward and reverse reads were linked using LinkGE allowing the calculation of recombination frequencies (Pham et al. 2021).

2.8 Graphs and statistical analyses

Graphs and statistical analyses were produced using Prism 9 (GraphPad) and assembled with Adobe Illustrator. Comparisons between groups were performed using paired *t*-test.

Table 1. Inactivating mutations introduced in the GFP coding region of HCV constructs.

Construct	GFP sequence (nt 55–65)	GFP sequence (nt 610–620)	GFP sequence (nt 660–670)
J6/JFH1	CTGGACGGCGA	ACCCAGTCCGC	CCTGCTGGAGT
J6/JFH1-MD0	CTGGACG**AT**GA	ACCCAGTCCGC	CCTGCTGGAGT
J6/JFH1-FD5	CTGGACGGCGA	ACCCAGT**TT**GC	CCTGCTGGAGT
J6/JFH1-FD6	CTGGACGGCGA	ACCCAGTCCGC	CCTGCTG**AA**T

Mutated nucleotides, relative to the GFP reference sequence, are indicated in bold.

3. Results

3.1 Development of a cell-based assay to measure HCV recombination

We developed an assay based on the HCV J6/JFH1 cell culture system to measure viral recombination using flow cytometry analysis, analogous to systems previously developed to study retroviral recombination in HIV (Rhodes et al. 2005; Galli et al. 2010; Rawson et al. 2018). The system utilizes the molecular markers flag tag and myc tag that can each be recognized by specific antibodies and GFP that can be detected directly by flow cytometry or microscopy. We generated two constructs based on the J6/JFH1 recombinant, J6/JFH1-FDG and J6/JFH1-MDG, containing either flag or myc tag fused to the N-terminus of HCV E2 envelope protein, respectively, and GFP inserted in the NS5A protein-coding region (Fig. 1A). Constructs used in the recombination assay were derived by modifying previously developed HCV J6/JFH1 cell culture systems, carrying GFP or flag tag (Gottwein et al. 2011; Prentoe and Bukh 2011).

We then introduced fluorescence-inactivating mutations close to the ends of the GFP region of both constructs, designed to abrogate fluorescence without disrupting the HCV reading frame. Each amino acid substitution was coded by at least two mutated nucleotides, to reduce the likelihood of reversion (Table 1). Mutation G20D was introduced in the J6/JFH1-MDG backbone, producing J6/JFH1-MD0 (referred to as MD0 in the text), whereas mutations S205F and E222K were introduced in the J6/JFH1-FDG backbone, producing J6/JFH1-FD5 and J6/JFH1-FD6, respectively (referred to as FD5 and FD6 in the text). The nucleotide distance between mutations at the two ends of GFP was 553 and 603 nucleotides, respectively, for MD0/FD5 and MD0/FD6 genome pairs. The introduced mutations were selected from a larger pool of mutations inserted in GFP-expressing plasmids, based on their location within the GFP coding region and their capacity to fully abrogate fluorescence without affecting expression of the GFP protein (Zacharias and Tsien 2006 and data not shown).

When individually present in Huh7.5 cells, the constructs MD0, FD5, and FD6 will produce a non-functional GFP protein and an E2 carrying their respective tag. However, when Huh7.5 cells contain combinations of MD0 and either FD5 or FD6, replication-driven recombination can occur between different HCV genomes in the GFP region, restoring a functional protein (Fig. 1B). The expression of flag tag, myc tag, and GFP can be scored by flow cytometry, allowing the enumeration of doubly infected and GFP-expressing cells, thus estimating HCV recombination rates for different marker distances.

3.2 Assessment and characterization of recombination constructs

All new constructs were confirmed by Sanger sequencing before being used to produce viral RNA by *in vitro* transcription. Viral RNA from each construct and adequate controls were transfected into Huh7.5 cells to verify viability and stability of the inserted sequences.

All constructs were viable after transfection and spread to most of the cell culture with no or only slight delay compared to J6/JFH1 (Fig. 2A). Infectivity titers of the virus supernatants collected at peak of infection spread showed values between 3.5 and 5 logs FFU/ml overall (Fig. 2B). Constructs carrying E2 tags only spread fast and reached the highest infectivity titers, whereas constructs carrying functional GFP in the NS5A region spread as fast but reached slightly lower peak titers. The constructs carrying GFP-inactivating mutation showed slower spread in cell culture and reached markedly lower infectivity titers, possibly due to an effect of the mutated GFP on NS5A stability or functionality.

Filter-sterilized peak-spread supernatants from transfections were then used to inoculate naïve Huh7.5 cells at 0.02 MOI. Infection spread was similar among constructs, with all viruses spreading to the entire cell culture between Day 4 and 7 post-infection (Fig. 2C). Peak infectivity titers were also similar across constructs, with values comprised between 4 and 5 logs FFU/ml (Fig. 2D).

Cells collected at peak of infection spread (Day 9) were plated on microscope slides, fixed, and stained with antibodies against flag tag, myc tag, and HCV core protein. Fluorescence microscopy images showed correct expression of the E2 tags for the tagged viruses co-localized with HCV core signal (Fig. 2E). Moreover, no GFP signal could be detected in cell infected by constructs carrying inactivating mutations, even after the cells had been infected for 9 days (Fig. 2E). In contrast, constructs MDG and FDG showed very clear GFP signal co-localized with HCV core and tags expression.

To further confirm that the inserts had been maintained, viral RNA was extracted from peak infection supernatants, amplified using an in-house developed protocol (Fahnøe and Bukh 2019), and subjected to Sanger sequencing. Consensus sequences confirmed the maintenance of tags and GFP regions and the presence of the mutations conferring GFP inactivation.

These results suggested that the inactivating mutations were stable and well tolerated by our viral constructs, at least for short-term experiments, and prompted us to proceed with the recombination assay.

3.3 HCV recombines efficiently during single-cycle replication

To estimate the baseline recombination frequency of HCV in cell culture, we co-transfected MD0 and FD6 RNA transcripts into S29 cells. Since this cell line lacks the main receptor for HCV, CD81, virions secreted by transfected cells cannot infect new cells, thus allowing the study of recombination during a single replication cycle.

Transfected cells were split at Day 3, 6, 8, and 10 post-transfection and analyzed by flow cytometry, as described in Materials and Methods. The expression of flag and myc tags was quantified to determine the proportion of singly infected and doubly infected cells, whereas the expression of GFP was used to determine the proportion of double-infected cells that produced recombinant genomes (Fig. 3A). The frequency of double-infected cells went from 14.4 per cent at Day 3 (SD = 6.4; $n = 3$) to 2.0 per cent at Day 10 (SD = 1.7; $n = 3$), consistent with the lack of re-infections after initial transfection (Fig. 3B). Conversely, the percentage of double-infected cells expressing a functional GFP went from 1.2 per cent at Day 3 (SD = 1.2; $n = 3$) to 6.7 per cent at Day 10 (SD = 2.9; $n = 3$), suggesting that continued replication of HCV genomes increases the likelihood of recombination within the GFP region. These results indicated that our system was able to reveal recombination between different HCV genomes using GFP as a surrogate marker.

However, while the rate of GFP-positive cells is indicative of ongoing viral recombination, it is not an adequate measure of viral recombination frequency, as multiple recombinant genomes can express GFP within the same cell. To better estimate the rate of HCV genetic recombination, we extracted viral RNA from culture supernatant and performed NGS analysis of the GFP region carried by released HCV virions. The presence or absence of GFP-inactivating mutations introduced at the ends of the GFP gene was evaluated and used to calculate the frequency of recombinant genomes released. The data revealed recombination frequencies within the GFP region of 7.6 per cent (SD = 1.6; $n = 3$) at Day 3, 6.4 per cent at Day 6 (SD = 0.5; $n = 3$), 6.2 at Day 8 (SD = 0.9; $n = 3$), and 4.3 at Day 10 (SD = 0.6; $n = 3$) (Fig. 3B). Interestingly, the frequencies of genomes with a GFP carrying both inactivating mutations, representing the opposite recombination event, were comparable to those obtained for functional GFP genomes: 9.0 per cent (SD = 0.7), 8.1 per cent (SD = 1.7), 6.8 per cent (SD = 1.5), and 4.7 per cent (SD = 1.9) for Day 3, 6, 8, and 10, respectively (data not shown). Controls including a 1:1 mixture of J6/JFH1-MD0 and J6/JFH1-FD6 RNA were processed together with culture samples and showed no occurrence of RT-PCR induced recombination in NGS, indicating that the detection of functional GFP by NGS was due to viral recombination.

Our results suggest that HCV genomes can reassort freely during replication in the infected cell, allowing for random recombination, and that measuring the frequency of reconstituted functional GFP is a valid surrogate for HCV recombination frequency estimation.

3.4 Recombination can occur between temporally separated infections

To further ascertain whether HCV genomes can freely reassort during replication, we performed modified co-transfection experiments where the MD0 and FD6 viruses were added 48 h apart. Huh7.5 cells were first transfected with either MD0 or FD6 virus, incubated for two days, and subsequently transfected with either FD6 or MD0, respectively. Although double-infection frequencies were overall below 1 per cent by flow cytometry analysis, NGS could detect recombinant genomes in the culture supernatants (Fig. 3C). Frequencies of recombinant genomes with reconstituted GFP were 5.2 per cent (Day 6), 2.1 per cent (Day 8), 1.3 per cent (Day 10), and 2.3 per cent (Day 13) for the MD0-to-FD6 transfection; 1.9 per cent (Day 6), 1.2 per cent (Day 8), 3.4 per cent (Day 10), and 3.9 per cent (Day 13) for the FD6-to-MD0 transfection. Although markedly lower than recombination frequencies measured in the standard co-transfection experiments, these data indicate that HCV genomes are not physically segregated during replication and can reassort with newly delivered molecules.

3.5 HCV recombination during full replication cycle

Overall, the data obtained in CD81-deficient Huh7 cells demonstrated that our system could detect and measure HCV recombination during a single infection cycle. To assess the recombination potential of HCV in a more physiological setting, we measured GFP reconstitution in a standard HCV cell culture system that allows infection and re-infection of target Huh7.5 cells.

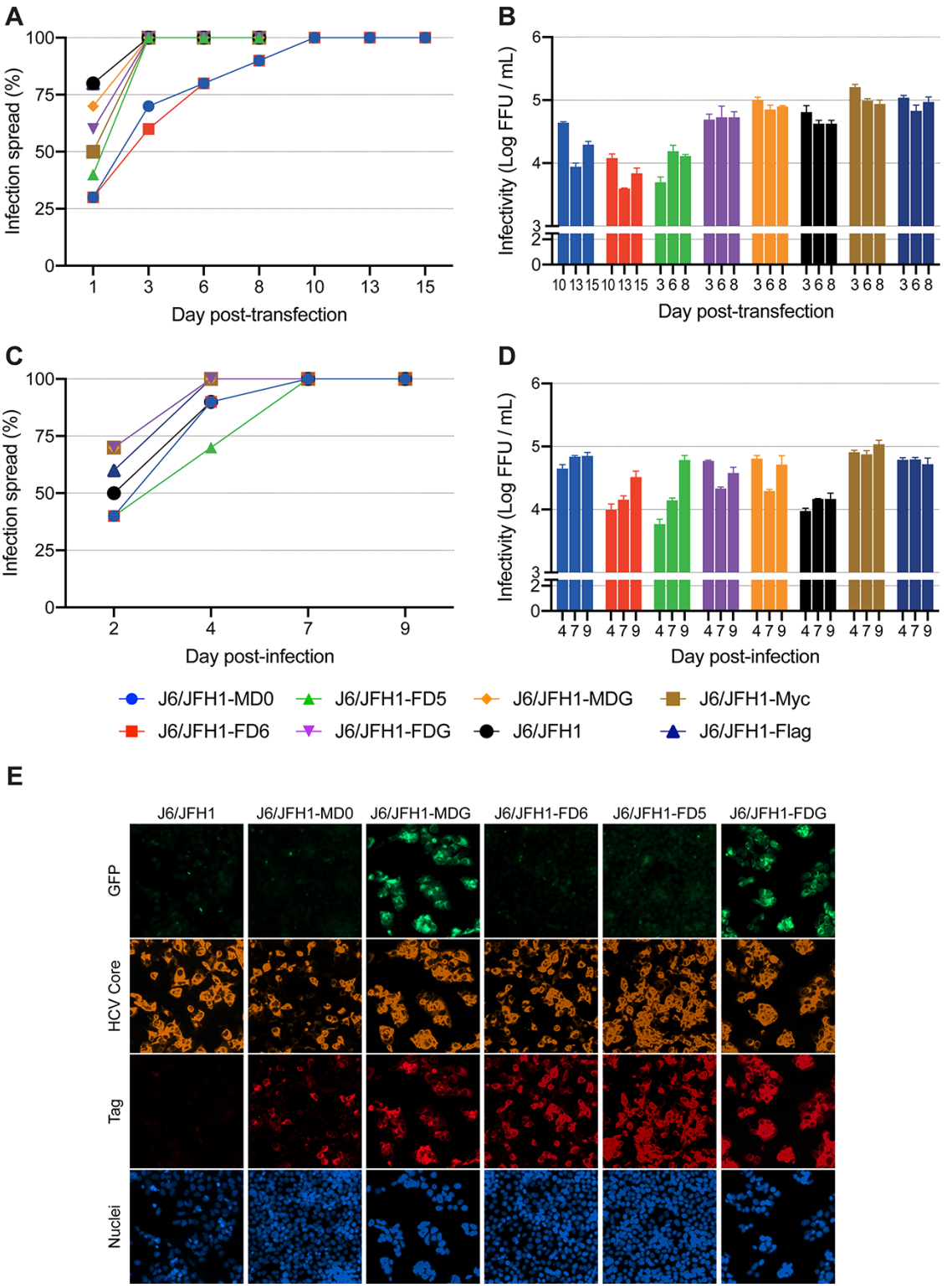

Figure 2. Characterization of viral constructs. The viral constructs represented in Fig. 1 were transfected in Huh7.5 cells and monitored for infection spread (A) and infectivity titers (B). Peak infection supernatants were subsequently used to infect naïve Huh7.5 cells at 0.02 MOI and monitored for spread (C) and infectivity titers (D). Colors and symbols are consistent across Panels A to D, and corresponding viruses are indicated in the legend. E) Infection spread and expression of tags and GFP were also assessed by fluorescent microscopy at Day 9 post-transfection, as described in Materials and Methods. GFP indicates GFP expression, HCV core shows signal from anti-Core antibody, tag displays signal from either anti-myc (for J6/JFH1-MD0 and -MDG) or anti-tag (for J6/JFH1-FD5, -FD6, and -FDG) antibodies, and nuclei indicate Hoechst counter staining.

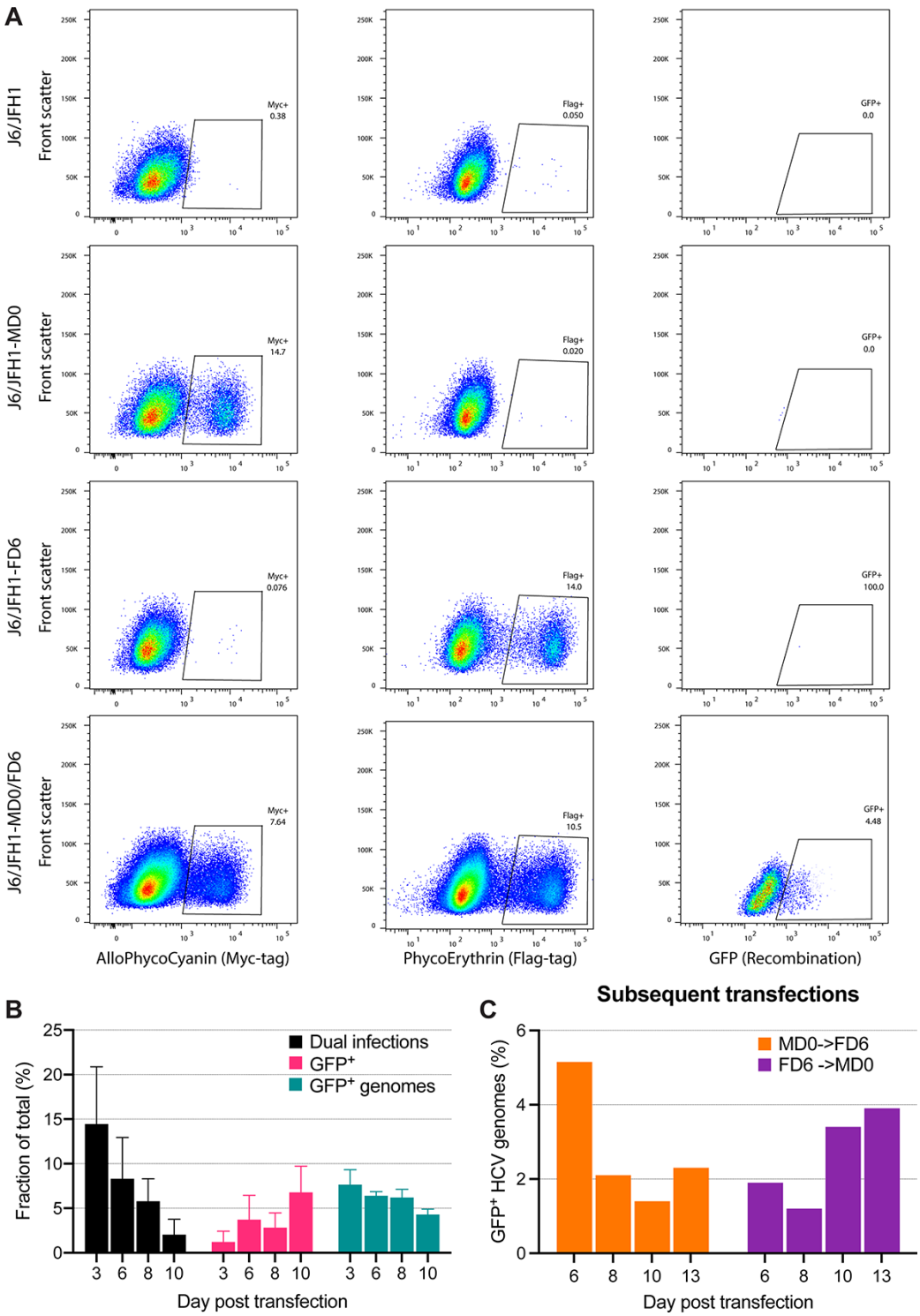

Figure 3. Detection of GFP reconstitution during transfection. A) Representative flow cytometry analysis of CD81-deficient S29 cells transfected with MD0 and FD6 constructs, either alone or in combination, and control J6/JFH1 virus. The first column shows myc-positive cells, resulting from MD0 infection; the middle column represents flag-positive cells, derived from FD6 infection; and the third column represents the intersection of myc- and flag-positive cells, representing double-infected cells, assayed for GFP expression, thus showing the fraction of double infections that resulted in the production of GFP-positive recombinants. B) Results of co-transfection experiments of MD0 and FD6 constructs analyzed by flow cytometry as depicted in Panel A. Black bars indicate double-infected cells (i.e. myc and flag positive); red bars represent GFP-positive cells among double-infected cells (i.e. myc, flag, and GFP positive). Supernatants from each time point were sequenced by NGS and the frequency of HCV genomes with reconstituted functional GFP gene was calculated, as indicated by the green bars. Bars represent mean of $n = 3$ experiments; error bars represent standard deviation. C) Results from subsequent transfection experiments, where constructs were transfected into target cells 48 h apart. Either MD0 or FD6 were first introduced into Huh 7.5 cells, followed 48 h later by either FD6 or MD0, respectively. Cell culture supernatants were analyzed as described for the co-transfection experiments and GFP reconstitution frequencies were calculated by NGS analysis.

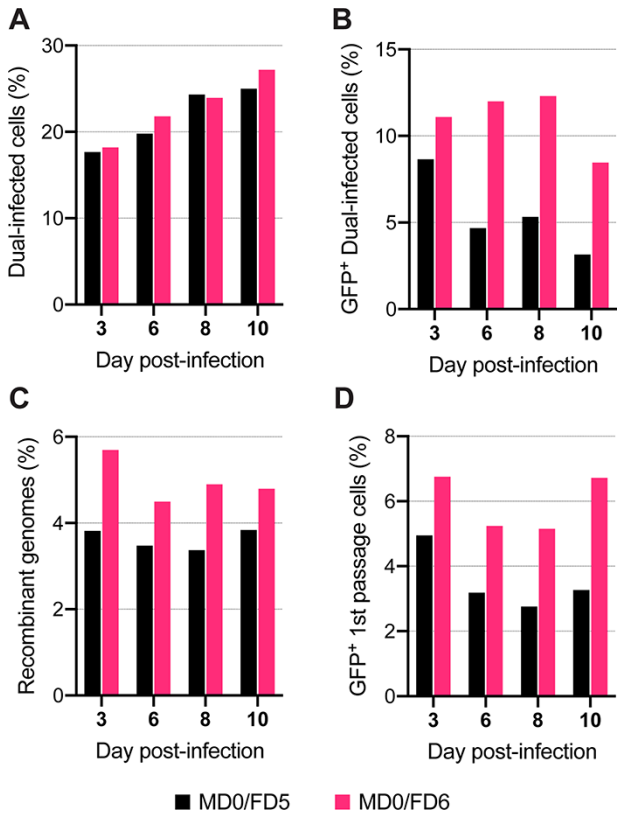

Figure 4. Detection of GFP reconstitution during infection. Huh7.5 cells were double-infected with MD0 and either FD5 or FD6 viruses at 0.1 MOI. A) Frequency of double-infected cells and B) GFP-positive double-infected cells were estimated by flow cytometry using the same analysis protocol used for transfections. C) Cell culture supernatants were analyzed at each time point by NGS to calculate the frequency of HCV genomes carrying functional GFP. D) Cell culture supernatants were used to perform short-term infections of naïve Huh7.5 cells and to calculate the fraction of GFP-positive infected cells. Color bars represent the same dual infection across panels, and the corresponding constructs are indicated in the legend.

Huh7.5 cells were co-infected with MD0 and FD6 viruses at 0.1 MOI; to also assess the contribution of marker distance to our ability of detecting GFP recombination, we co-infected Huh7.5 cells with MD0 and FD5 viruses. Using a protocol similar to the co-transfection experiments, we split cells at Days 3, 6, 8, and 10 and performed flow cytometry analysis at all time points. Double infections rates were similar for the MD0/FD6 and MD0/FD5 experiments, slightly increasing over time from about 18 per cent to about 25 per cent for both cultures (Fig. 4A). The rate of GFP-positive cells among double-infected cells was significantly higher ($P = 0.016$; t-test) for the MD0/FD6 co-infection compared to the MD0/FD5 culture, at all analyzed time points (Fig. 4B). These results suggest that the greater distance between GFP-inactivating mutations in the MD0/FD6 co-infection increases the chance of recombination events between them compared to the MD0/FD5 co-infection.

To confirm this hypothesis, we performed NGS analysis of the GFP region obtained from viral supernatants. The frequencies of HCV genomes with functional GFP were significantly higher for the MD0/FD6 compared to the MD0/FD5 co-infection at all time points (Fig. 4C), averaging at 5.0 per cent for the former and 3.6 per cent for the latter ($P = 0.008$; t-test). To further confirm GFP reconstitution frequencies in HCV recombinants, naïve Huh7.5 cells were infected for 4 h with viral supernatants from all time points of both cultures, incubated for 48 h and analyzed by flow cytometry for GFP expression. Given the short infection and incubation time, most infected cells would be produced by individual HCV infections. Recombinant virus derived from MD0/FD6 produced GFP signal in 5.9 per cent of infected cells, on average, whereas the fraction of GFP-positive cells was 3.5 per cent in infections from MD0/FD5 recombinants (Fig. 4D). Similar to the NGS data, the difference in GFP recombination rates between MD0/FD6 and MD0/FD5 calculated by first passage infection was statistically significant ($P = 0.007$; t-test). Taken together, these data indicate that recombination between MD0 and either FD5 or FD6 viruses produced viable recombinants carrying functional GFP proteins and shows that the distance between inactivating mutations within the GFP region affects the likelihood of detecting recombination events.

3.6 Calculation of recombination rates

To better compare recombination rates between experiments and to other viruses, we converted recombination rates to %MDR, as previously described for HIV-1 (Rhodes et al. 2005). Assuming random assortment of HCV genomes within the cell, as supported by our experiments, recombination events can occur between any random pair of genomes. For MD0/FD6 experiments these correspond to MD0/MD0, FD6/FD6, MD0/FD6, and FD6/MD0 pairs. Only the latter two kinds of events, representing 50 per cent of all possible events, can lead to GFP reconstitution. Our assay will result in reconstitution of a functional GFP if any odd number of recombination events occurs within the GFP region comprised between the inactivating mutations. Given the comparatively limited length of such region, we assume that most recombination events will be singular and only a minority of genomes will contain multiple recombination events within the GFP gene. This allows us to simplify the frequency calculation by considering recombination events as single occurrences for the purpose of this analysis. Furthermore, assuming random distribution of recombination sites across the HCV genome, these events can result in one of four possible scenarios with respect to the GFP region: GFP with inactivating mutations from either MD0 or FD6, GFP with both inactivating mutations, and GFP without inactivating mutations. Only the latter will produce a GFP signal upon recombination and be detectable in our system, thus representing 12.5 per cent ($\frac{50\%}{4}$) of all possible recombination events. We thus define the percentage of maximum detectable recombination (%MDR) as $\frac{GFPrec\%}{12.5\%} * 100$, which provides an estimate of the fraction of recombination detectable in our assay relative to the theoretical maximum measurable frequency at saturating recombination rates.

We calculated mean GFP recombination rates of each co-transfection and co-infection experiments, by averaging rates measured at each time point. For the co-infection experiments, we considered rates obtained by NGS and first passage infection independently (Table 2). The analysis revealed %MDR between 40 per cent and 49 per cent for MD0/FD6 recombination experiments, and %MDR around 28 per cent for MD0/FD5. These results suggest that HCV recombines at high frequency between almost identical genomes, reaching almost 50 per cent of maximum recombination frequencies between markers spaced about 603 nucleotides apart and of about 30 per cent for markers closer together (553 bp). Moreover, given the assumptions described above regarding the occurrence of multiple recombination events within the observed

Table 2. Calculation of recombination frequencies.

Experiment	GFP (%)[a]	MDR (%)[b]	Norm[c]
Co-transfection NGS			
J6/JFH1-MD0/J6/JFH1-FD6	6.1	49.0	1.0×10^{-4}
Co-infection NGS			
J6/JFH1-MD0/J6/JFH1-FD6	5.0	40.0	8.3×10^{-5}
J6/JFH1-MD0/J6/JFH1-FD5	3.6	28.8	6.5×10^{-5}
Co-infection first passage			
J6/JFH1-MD0/J6/JFH1-FD6	5.9	47.2	9.8×10^{-5}
J6/JFH1-MD0/J6/JFH1-FD5	3.5	28.0	6.3×10^{-5}

[a]Mean GFP recombination frequency.
[b]Maximum detectable recombination.
[c]Normalized recombination frequency expressed as recombination events per nucleotide.

region, this should be considered a minimum estimate of recombination frequency as few multiple instances of recombination could have been counted as single events.

In addition, under the assumption that recombination frequency is constant across the genome, normalized recombination frequencies can be calculated by dividing the GFP recombination frequency by the distance between GFP markers (Table 2). Normalized recombination was about 1×10^{-4} and 6×10^{-5} events/nucleotide for MD0/FD6 and MD0/FD5 pairs, respectively. Since normalized recombination should be comparable across differently sized regions unless restraints are present, our data suggest that the frequency of recombination within the analyzed GFP region might not be constant. Whether such variation of recombination frequency is reflected in the HCV genome remains to be determined.

4. Discussion

In this study we describe the development of a system to examine the recombination rate of HCV, based on the detection of proteins expression by flow cytometry. The assay can score large amounts of cells, thus allowing high-throughput analysis, and produce quantitative estimates of recombination rates. In addition, our system is flexible and can be used with different Huh7-derived cell lines (such as Huh7.5 and S29) and under differential experimental conditions, allowing investigation of the factors that influence recombination in HCV. To the best of our knowledge, this is the first such assay developed for the study of HCV or other members of the *Flaviviridae* family of viruses.

For the assay to work properly, replication and expression of the two recombining genomes need to be comparable, since excess of one genome over the other would reduce the observable frequency of recombination events. Culture spread of the viral constructs developed for this study showed that the constructs carrying mutated GFP genes had slower spread kinetics and lower infectivity titers, compared to their counterparts carrying functional GFP. The observed differences in spread could be due to an effect of the inactivating GFP mutations on the NS5A stability. However, constructs carrying mutated GFP had comparable spread kinetics, indicating similar replication capacity and thus fulfilling the assay requirement.

Normalized recombination rates can be calculated for comparison with studies in other virus systems, under the assumption that recombination frequency is equal across viral genomes. Previous *in vitro* studies of HCV examined recombination between defective replicons to estimate crossover frequencies and found that HCV recombines at frequencies of 4×10^{-8} crossovers/nucleotide (Reiter et al. 2011). In a later study, we demonstrated that HCV could recombine through both replicative and non-replicative recombination using reconstitution of viable genome as indication of recombination between non-functional genomes (Scheel et al. 2013). The system used was not designed to produce quantitative information regarding frequencies, thus the recombination rates could only be roughly estimated at 4.9×10^{-9} crossovers/nucleotide. These estimates were much lower than *in vitro* estimates for other viruses such as HIV-1 (1.5×10^{-4} crossovers/nucleotide) and polio virus (7×10^{-6} crossovers/nucleotide) (Kirkegaard and Baltimore 1986; Rhodes et al. 2005), although essential differences in the detection systems invite caution in making comparisons, suggesting a lower intrinsic recombination frequency of HCV. However, the reported rates were also lower than previous *in vivo* estimates of HCV recombination obtained in experimentally infected chimpanzees (3×10^{-5} crossovers/nucleotide) (Gao et al. 2007), suggesting that the detection systems used were not properly recapitulating HCV recombination *in vitro*.

In the present study, we estimate HCV recombination frequencies of around 1×10^{-4} crossovers/nucleotide for markers spaced at about 600 nucleotides and of around 6×10^{-5} crossovers/nucleotide for markers spaced at about 550 nucleotides, which represent recombination rates comparable to those observed in retroviruses. It is also worth noting that since our system cannot discriminate between viruses produced by double- or single-infected cells, these values are likely underestimates of actual recombination frequencies. The calculated frequencies are compatible with the reported *in vivo* frequency of 3×10^{-5} crossovers/nucleotide (Gao et al. 2007), as it can be assumed that some recombinant selection will be ongoing *in vivo* thus resulting in lower frequencies overall. A high intrinsic recombination capacity of HCV is also consistent with reports detecting high frequency of intra-patient recombinant strains in the absence of superinfection (Sentandreu et al. 2008), a situation in which recombinant selection would be arguably low due to the similarity among strains. The elevated values of %MDR further indicate that HCV can recombine at high rates. For the 600-nucleotide window, %MDR values approach 50 per cent, showing that roughly half of possible recombination events are happening within this region. HIV-1, a highly recombinogenic virus, displays similar recombination frequencies for intra-marker regions of comparable size (Rhodes et al. 2005).

Detection of recombination events with selection markers is known to be affected by the distance between markers, with lower recombination rates associated with shorter distances (Rhodes et al. 2005; Reiter et al. 2011). Our data show a reduction of recombination frequencies when using constructs with reduced distance between markers, confirming previous reports for HCV and other viruses. However, the reduction observed in our MD0/FD5 experiments is higher than expected, as its normalized frequency is nonlinear with the measurements obtained with the MD0/FD6 pair. This could be explained by the slightly slower replication kinetics of FD5 that would result in unequal concentration of this virus compared to MD0. The steep reduction in GFP-positive dual infections in the MD0/FD5 experiments partly corroborates this hypothesis, indicating that evaluations at Day 3 post-infection could provide the better estimates of recombination. Another explanation could be that recombination rates are variable within the GFP region, so that the shorter MD0/FD5 region contains areas of lower intrinsic recombination capacity. The distribution of recombination frequencies within the HCV genomes remains to be investigated, and the frequencies measured by our GFP reconstitution assays might not entirely reflect native HCV

recombination. Further experiments will be necessary to clarify this issue.

We have developed an efficient system to quantify HCV recombination, revealing that HCV can recombine at high frequency in the absence of selective pressure. Our findings support the hypothesis that the low frequency of identified CRFs is due to strong selection against most recombinants rather than low intrinsic recombination capability. The structure of most identified HCV CRFs involved crossovers in the NS2–NS3 junction region, implying that recombination of whole structural and nonstructural genomic fragments is more likely to result in viable and fit viruses. This lends support to the idea that recombinants with crossovers at other genomic locations are heavily counterselected, due to their lower fitness, and thus are not observed in the viral population. Results of several *in vitro* studies artificially producing HCV intra- and inter-genotypic recombinants, in which extensive adaptation was required for the recombinants to be viable in cell culture (Ramirez and Bukh 2018), are consistent with these observations. The novel assay described here can be further utilized to investigate HCV recombination between more divergent strains, clarifying the impact of recombination on HCV evolution and escape from antiviral or immune pressure.

Acknowledgements

We thank Anna-Louise Sørensen and Lotte Mikkelsen (Department of Infectious Diseases, Hvidovre Hospital) and Louise B. Christensen (Department of Clinical Microbiology, Hvidovre Hospital) for laboratory assistance, and Bjarne Ørskov Lindhardt (Department of Infectious Diseases, Hvidovre Hospital) and Carsten Geisler (University of Copenhagen) for valuable support.

Funding

This study was supported by grants from Independent Research Fund Denmark (A.G. and J.B.), the Danish Cancer Society (J.B.), the Weimann Foundation (U.F.), and the Novo Nordisk Foundation (J.B.). The funders had no role in the study design, data collection and analysis, decision to publish, or preparation of the manuscript.

Conflict of interest: None declared.

Data availability

The data analyzed and presented in this study are available on request from the corresponding authors.

References

Baroth, M. et al. (2000) 'Insertion of Cellular NEDD8 Coding Sequences in a Pestivirus', *Virology*, 278: 456–66.

Bhattacharya, D. et al. (2011) 'Naturally Occurring Genotype 2b/1a Hepatitis C Virus in the United States', *Virology Journal*, 8: 458.

Borgia, S. M. et al. (2018) 'Identification of a Novel Hepatitis C Virus Genotype from Punjab, India: Expanding Classification of Hepatitis C Virus into 8 Genotypes', *The Journal of Infectious Diseases*, 218: 1722–9.

Bukh, J. (2016) 'The History of Hepatitis C Virus (HCV): Basic Research Reveals Unique Features in Phylogeny, Evolution and the Viral Life Cycle with New Perspectives for Epidemic Control', *Journal of Hepatology*, 65: S2–21.

Calado, R. A. et al. (2011) 'Hepatitis C Virus Subtypes Circulating among Intravenous Drug Users in Lisbon, Portugal', *Journal of Medical Virology*, 83: 608–15.

Chang, W. et al. (2020) 'HIV-1 Genetic Diversity and Recombinant Forms among Men Who Have Sex with Men at a Sentinel Surveillance Site in Xi'an City, China', *Infection, Genetics and Evolution*, 81: 104257.

Colina, R. et al. (2004) 'Evidence of Intratypic Recombination in Natural Populations of Hepatitis C Virus', *Journal of General Virology*, 85: 31–7.

Cristina, J., and Colina, R. (2006) 'Evidence of Structural Genomic Region Recombination in Hepatitis C Virus', *Virology Journal*, 3: 53.

Fahnøe, U., and Bukh, J. (2019) 'Full-Length Open Reading Frame Amplification of Hepatitis C Virus', *Methods in Molecular Biology (Clifton, N.J.)*, 1911: 85–91.

Fricke, J., Gunn, M., and Meyers, G. (2001) 'A Family of Closely Related Bovine Viral Diarrhea Virus Recombinants Identified in an Animal Suffering from Mucosal Disease: New Insights into the Development of A Lethal Disease in Cattle', *Virology*, 291: 77–90.

Galli, A. et al. (2010) 'Patterns of Human Immunodeficiency Virus Type 1 Recombination Ex Vivo Provide Evidence for Coadaptation of Distant Sites, Resulting in Purifying Selection for Intersubtype Recombinants during Replication', *Journal of Virology*, 84: 7651–61.

Galli, A. et al. (2018) 'Antiviral Effect of Ribavirin against HCV Associated with Increased Frequency of G-to-A and C-to-U Transitions in Infectious Cell Culture Model', *Scientific Reports*, 8: 4619.

Galli, A., and Bukh, J. (2014) 'Comparative Analysis of the Molecular Mechanisms of Recombination in Hepatitis C Virus', *Trends in Microbiology*, 22: 354–64.

Galli, A., Ramirez, S., and Bukh, J. (2021) 'Lipid Droplets Accumulation during Hepatitis C Virus Infection in Cell-Culture Varies among Genotype 1-3 Strains and Does Not Correlate with Virus Replication', *Viruses*, 13: 3.

Gao, F. et al. (2007) 'Recombinant Hepatitis C Virus in Experimentally Infected Chimpanzees', *Journal of General Virology*, 88: 143–7.

Gottwein, J. M. et al. (2011) 'Development and Application of Hepatitis C Reporter Viruses with Genotype 1 to 7 Core-nonstructural Protein 2 (NS2) Expressing Fluorescent Proteins or Luciferase in Modified JFH1 NS5A', *Journal of Virology*, 85: 8913–28.

Hoshino, H. et al. (2012) 'Inter-genotypic Recombinant Hepatitis C Virus Strains in Japan Noted by Discrepancies between Immunoassay and Sequencing', *Journal of Medical Virology*, 84: 1018–24.

Jensen, S. B. et al. (2019) 'Evolutionary Pathways to Persistence of Highly Fit and Resistant Hepatitis C Virus Protease Inhibitor Escape Variants', *Hepatology*, 70: 771–87.

Kageyama, S. et al. (2006) 'A Natural Inter-genotypic (2b/1b) Recombinant of Hepatitis C Virus in the Philippines', *Journal of Medical Virology*, 78: 1423–8.

Kalinina, O. et al. (2002) 'A Natural Intergenotypic Recombinant of Hepatitis C Virus Identified in St. Petersburg', *Journal of Virology*, 76: 4034–43.

Kirkegaard, K., and Baltimore, D. (1986) 'The Mechanism of RNA Recombination in Poliovirus', *Cell*, 47: 433–43.

Lai, M. M. (1992) 'RNA Recombination in Animal and Plant Viruses', *Microbiological Reviews*, 56: 61–79.

Lee, Y. M. et al. (2010) 'Molecular Epidemiology of HCV Genotypes among Injection Drug Users in Taiwan: Full-length Sequences of Two New Subtype 6w Strains and a Recombinant Form_2b6w', *Journal of Medical Virology*, 82: 57–68.

Legrand-Abravanel, F. et al. (2007) 'New Natural Intergenotypic (2/5) Recombinant of Hepatitis C Virus', *Journal of Virology*, 81: 4357–62.

Lindenbach, B. D. et al. (2005) 'Complete Replication of Hepatitis C Virus in Cell Culture', *Science*, 309: 623–6.

Mejer, N. et al. (2020) 'Mutations Identified in the Hepatitis C Virus (HCV) Polymerase of Patients with Chronic HCV Treated with Ribavirin Cause Resistance and Affect Viral Replication Fidelity', *Antimicrobial Agents and Chemotherapy*, 64: e01417–20.

Moreno, P. et al. (2009) 'Evidence of Recombination in Hepatitis C Virus Populations Infecting a Hemophiliac Patient', *Virology Journal*, 6: 203.

Noppornpanth, S. et al. (2006) 'Identification of a Naturally Occurring Recombinant Genotype 2/6 Hepatitis C Virus', *Journal of Virology*, 80: 7569–77.

Paprotka, T. et al. (2011) 'Recombinant Origin of the Retrovirus XMRV', *Science*, 333: 97–101.

Pham, L. V. et al. (2021) 'HCV Genome-wide Analysis for Development of Efficient Culture Systems and Unravelling of Antiviral Resistance in Genotype 4', *Gut* 08 Apr 2021.

Prentoe, J., and Bukh, J. (2011) 'Hepatitis C Virus Expressing Flag-tagged Envelope Protein 2 Has Unaltered Infectivity and Density, Is Specifically Neutralized by Flag Antibodies and Can Be Purified by Affinity Chromatography', *Virology*, 409: 148–55.

Rambaut, A. et al. (2004) 'The Causes and Consequences of HIV Evolution', *Nature Reviews Genetics*, 5: 52–61.

Ramirez, S., and Bukh, J. (2018) 'Current Status and Future Development of Infectious Cell-culture Models for the Major Genotypes of Hepatitis C Virus: Essential Tools in Testing of Antivirals and Emerging Vaccine Strategies', *Antiviral Research*, 158: 264–87.

Rawson, J. M. O. et al. (2018) 'Recombination Is Required for Efficient HIV-1 Replication and the Maintenance of Viral Genome Integrity', *Nucleic Acids Research*, 46: 10535–45.

Reiter, J. et al. (2011) 'Hepatitis C Virus RNA Recombination in Cell Culture', *Journal of Hepatology*, 55: 777–83.

Rhodes, T. D. et al. (2005) 'Genetic Recombination of Human Immunodeficiency Virus Type 1 in One Round of Viral Replication: Effects of Genetic Distance, Target Cells, Accessory Genes, and Lack of High Negative Interference in Crossover Events', *Journal of Virology*, 79: 1666–77.

Ross, R. S. et al. (2008) 'Evidence for a Complex Mosaic Genome Pattern in a Full-length Hepatitis C Virus Sequence', *Evolutionary Bioinformatics*, 4: 249–54.

Russell, R. S. et al. (2008) 'Advantages of a Single-cycle Production Assay to Study Cell Culture-adaptive Mutations of Hepatitis C Virus', *Proceedings of the National Academy of Sciences*, 105: 4370–5.

Scheel, T. K. et al. (2013) 'Productive Homologous and Non-homologous Recombination of Hepatitis C Virus in Cell Culture', *PLoS Pathogens*, 9: e1003228.

Sentandreu, V. et al. (2008) 'Evidence of Recombination in Intrapatient Populations of Hepatitis C Virus', *PLoS One*, 3: e3239.

Shi, W. et al. (2012) 'Recombination in Hepatitis C Virus: Identification of Four Novel Naturally Occurring Inter-subtype Recombinants', *PLoS One*, 7: e41997.

Smith, D. B. et al. (2014) 'Expanded Classification of Hepatitis C Virus into 7 Genotypes and 67 Subtypes: Updated Criteria and Genotype Assignment Web Resource', *Hepatology*, 59: 318–27.

Stapley, J. et al. (2017) 'Recombination: The Good, the Bad and the Variable', *Philosophical Transactions of the Royal Society B: Biological Sciences*, 372: 20170279.

Uzcategui, N. Y. et al. (2001) 'Molecular Epidemiology of Dengue Type 2 Virus in Venezuela: Evidence for in Situ Virus Evolution and Recombination', *Journal of General Virology*, 82: 2945–53.

Worobey, M., and Holmes, E. C. (1999) 'Evolutionary Aspects of Recombination in RNA Viruses', *Journal of General Virology*, 80: 2535–43.

Worobey, M., and Holmes, E. C. (2001) 'Homologous Recombination in GB Virus C/hepatitis G Virus', *Molecular Biology and Evolution*, 18: 254–61.

Worobey, M., Rambaut, A., and Holmes, E. C. (1999) 'Widespread Intra-serotype Recombination in Natural Populations of Dengue Virus', *Proceedings of the National Academy of Sciences*, 96: 7352–7.

Yokoyama, K. et al. (2011) 'Identification and Characterization of a Natural Inter-genotypic (2b/1b) Recombinant Hepatitis C Virus in Japan', *Archives of Virology*, 156: 1591–601.

Zacharias, D. A., and Tsien, R. Y. (2006) 'Molecular Biology and Mutation of Green Fluorescent Protein', *Methods of Biochemical Analysis*, 47: 83–120.

Zhang, X. W., Yap, Y. L., and Danchin, A. (2005) 'Testing the Hypothesis of a Recombinant Origin of the SARS-associated Coronavirus', *Archives of Virology*, 150: 1–20.